Renewable Energy 216 (2023) 119056

Contents lists available at ScienceDirect

Renewable Energy

journal homepage: www.elsevier.com/locate/renene

Exploring flood and erosion risk indices for optimal solar PV site selection and assessing the influence of topographic resolution

Kutay Yılmaz [a,*], Ali Ersin Dinçer [b], Elif N. Ayhan [c]

[a] ORCAS Engineering & Consultancy Co., Ankara, 6510, Turkey
[b] Dep. of Civil Eng., Hydraulics Laboratory, Abdullah Gül University, Kayseri, 38080, Turkey
[c] Dept. of Urban Planning, Istanbul Metropolitan Municipality, Istanbul, 34134, Turkey

ARTICLE INFO

Keywords:
Renewable energy
Solar PV site selection
Analytical Hierarchy Process (AHP)
Multi-Criteria Decision-Making (MCDM)
Flood
Erosion

ABSTRACT

This study explores the suitability of Menteşe Region in Türkiye for the installation of solar PV farms, given the significant increase in energy demand in the country and the need to reduce reliance on fossil fuels. The Analytical Hierarchy Process (AHP) method, which has been widely used in previous studies, is employed to identify the most influential criteria for site selection, including environmental, economic, and social factors. However, this study introduces two new factors, flood hazard and erosion indices, to the analysis, which are crucial in areas susceptible to these hazards. The results show that approximately 7.5% of the study surface area is suitable for solar PV production. The study reveals that flood hazard and erosion indices have an effect on the suitable sites despite their relatively lower weights in the AHP. In addition, the study illustrates that site selection can be carried out using topographic data of lower resolution, as long as the data is resampled to match the resolution of land use data. The study is novel in its integration of flood and erosion risk indices in the decision process and its investigation of the influence of topographic resolution on site selection for solar PV panels.

1. Introduction

Energy is a critical element for the advancement of society, with increasing energy consumption being driven by the rise in global population and the industrialization of many countries. The primary energy production, accounting for more than 80% of the total, is derived from fossil fuels [1]. However, the distribution of fossil fuel reserves across the globe is uneven and limited, which implies that economic and political conflicts are likely to ensue in the foreseeable future [2]. Additionally, climate change driven by burning fossil fuels causes damage to ecosystems and economies of several nations. To limit global warming due to climate change, the Paris Agreement was adopted in 2015. According to the agreement, all countries, including 194 states and EU that represents approximately 98% of globally emitted greenhouse gases, are committed to reduce their emissions regarding their total emission share [3]. Accordingly, many countries submitted Nationally Determined Contributions (NDCs) outlining their emission reduction targets and strategies [4] and they revised their NDCs to increase their ambition in subsequent years. Additionally, efforts to mobilize climate finance, including the establishment of the Green Climate Fund, were strengthened [5]. Global stocktaking processes were established [6]. Annual UN climate conferences (COP) continue to serve as important platforms for collaboration and monitoring progress. These developments reflect ongoing efforts to address climate change and implement the commitments made under the Paris Agreement.

Environmental concerns and the surge in energy prices have resulted in a growing demand for renewable energy sources, which provide a more sustainable and eco-friendly solution [7]. In essence, the current energy supply system, which primarily relies on fossil fuels, should be replaced with a system based on renewable energy [8]. Compared to other sources of energy, the adverse effects of renewable energy sources on the environment are minimal, and these sources are inexhaustible. Hydro, wind, and solar power are the most widely used renewable energy sources for power generation [9]. Additionally, significant advancements in policies supporting the development of bioenergy, leading to an unexpected 8% increase in energy generation from biomass between 2019 and 2020, surpassing the projected 7% rise were observed (IEA, 2022b). Furthermore, in 2021, solar photovoltaic (PV) generation increased by approximately 22% throughout the world, marking the second largest growth of all renewable energy technologies [10]. This growth is attributable to the efforts of developed nations, with China, the United States, and the European Union accounting for the

* Corresponding author.
E-mail addresses: ktyylmz@gmail.com (K. Yılmaz), ersin.dincer@agu.edu.tr (A.E. Dinçer), elifayhan7560@gmail.com (E.N. Ayhan).

https://doi.org/10.1016/j.renene.2023.119056
Received 14 March 2023; Received in revised form 8 July 2023; Accepted 17 July 2023
Available online 20 July 2023

most substantial increase in solar power generation, at 38%, 17%, and 10%, respectively. Solar PV is the third largest renewable energy technology behind hydropower and wind [11].

Parallel to the global increase in energy demand, the annual gross electricity consumption of Türkiye increased by 8.74% in 2021 [12]. The sources of electricity generation comprised natural gas (33.2%), coal (30.9%), hydropower (16.7%), wind (9.4%), solar (4.2%), geothermal (3.2%), and other sources (2.4%) in the same year. Despite Türkiye's abundant solar energy potential, the share of solar energy in the country's electricity mix remains relatively low. Specifically, Türkiye receives 1.02 million TWh of solar radiation annually, yet the solar power generation amounts to only 12.8 TWh per year [13]. In addition, 63% of country's surface area is technically and economically appropriate for the solar power production [14]. Given the significant gap between Türkiye's solar energy potential and its installed solar capacity, the installation of new solar PV farms in various regions is expected.

Site selection for solar power systems plays an important role for optimal energy production. While annual solar radiation is a crucial factor, it is also essential to consider environmental, economic, and social factors in determining suitable solar PV locations. Thus, the selection of ideal PV sites requires the evaluation of various criteria. Multi-Criteria Decision-Making Techniques (MCDMs) have been employed to analyze different parameters and determine the location of PV systems. The Analytical Hierarchy Process (AHP) is one of the most widely used MCDMs for this purpose [15]. Previous studies have applied AHP to optimal site selection for solar PV. For instance, a study conducted in Eastern Morocco [16] used the AHP method by choosing four criteria, including climate, orography, water resource and location, as well as eight sub criteria, to locate suitable sites for PV farms. Their AHP weight analysis showed that the climate criterion was the most influential with a weight of 59%. They found that 19% of Eastern Morocco's surface was highly suitable for PV, whereas unsuitable sites represented 15%. The percentage of suitable areas in Eastern Morocco was relatively high compared to other case studies conducted in regions such as İzmir, Türkiye [17], Karapınar, Türkiye [9], Granada, Spain [18] and Murcia, Spain [19].

Similarly, a study conducted in southern Morocco [20] investigated the suitable location for a solar farm using AHP. They selected four main criteria, including location, orography, land use, and climate in AHP. Their AHP weight analysis suggested that the climate criterion had the highest weight of 59%, which was the same as the AHP weight analysis results in the Eastern Morocco study. The dominance of orography and location was 25% and 5%, respectively, compared to 23.5% and 5.7% in the Eastern Morocco study. They did not include water resource as a criterion, which was the main difference from the Eastern Morocco study. According to their results, 19% of southern Morocco was highly suitable for PV farms.

In another study conducted in Karapınar, Konya, Türkiye [9], the AHP method was used to determine the suitable site for solar farms. They selected five criteria, including distance from residential areas (13.75%), land use (41.25%), distance from roads (3.20%), slope (8.10%) and distance from transmission lines (33.70%). Notably, solar radiation, which is the most dominant criterion in many studies [16,20], was not included in the criteria list. The percentage of highly suitable areas for solar farms was found to be 13.92%, while 40.34% of the investigated area was unsuitable for solar farms.

In a study conducted in Malatya, Türkiye [21], AHP was used to find the suitable locations of PV. They used 11 criteria in the AHP method, which led to a lower percentage of suitable areas. A list of the AHP criteria used in previous studies is given in Table 1. As can be seen the selection of the criteria is case-specific and changes mainly with geographical location.

Various criteria have been used in previous studies to determine suitable locations for solar power plants. While natural hazards such as earthquakes have been included in the criteria list by considering distance to fault lines, no comprehensive study has been found where natural hazards are included in the criteria list by considering hazard indices. Therefore, the main objective of this study is to determine suitable locations for solar power plants by incorporating flood hazard and erosion risk indices into the criteria list. To the best of the authors' knowledge, this is the first study to examine the effect of floods and erosion in the site selection of solar power plants. Additionally, a sensitivity analysis is performed to investigate the impact of different Digital Elevation Models (DEMs) on the results.

The inclusion of flood hazard and erosion risk indices in the criteria list offers a more comprehensive and realistic approach for determining suitable locations for solar power plants. This approach takes into account the increasing trend of hydrological extremes caused by global warming. As global warming continues, the world is experiencing more frequent and destructive floods, as well as excess precipitation that can contribute to erosion [28]. By considering these factors, the site selection process can address the potential challenges posed by these hydrological risks and ensure the long-term viability and resilience of solar power installations. Furthermore, understanding the sensitivity of the results to different DEM resolutions can provide valuable information for decision-makers and increase confidence in the accuracy of the site selection process. In summary, this study seeks to fill a gap in the literature by incorporating flood hazard and erosion risk indices in the site selection process for solar power plants, and by examining the impact of different DEM resolutions on the results.

2. Methodology

2.1. Study area

The Menteşe District of Muğla Province, situated in the southwest of Türkiye, has been chosen as the study area due to several reasons. Firstly, the area exhibits a high solar potential, making it suitable for solar power plant installation. Additionally, the region experiences excess precipitation, leading to a long-term average precipitation of 1165.2 mm, which indicates a higher flood risk compared to the national

Table 1
Criteria list used in previous studies.

Criterion	[18]	[22]	[9]	[20]	[23]	[24]	[25]	[16]	[26]	[21]	[7]	[27]
Solar energy potential (solar radiation + LST)	x	x		x	x	x	x	x	x	x	x	x
Orography (slope + aspect)	x		x	x		x	x	x	x	x	x	x
NDVI						x	x		x			
Distance from cities	x		x	x	x		x	x	x	x	x	x
Land use and cover			x	x			x			x	x	x
Annual average rainfall									x			
Distance from roads	x	x	x	x	x		x	x		x	x	x
Distance from transmission lines			x				x	x		x	x	x
Distance from transformation centers					x					x	x	
Distance from water bodies								x		x	x	

average of 618.9 mm for Türkiye [55]. Furthermore, the region is known for its diverse topography and land use patterns, including agricultural areas and protected natural landscapes, providing a varied terrain to assess the impact of floods and erosion on the site selection of solar PV panels. Muğla is renowned for its warm climate and is a popular tourist destination due to its picturesque beaches and historic sites. The spatial location of the district is given in Fig. 1.

2.2. AHP method

The Analytical Hierarchy Process (AHP) is a widely used multi-criteria decision-making method that is particularly favored by researchers and practitioners alike. It enables the conversion of subjective preferences into a set of tangible mathematical problems, with the aid of expert opinion. AHP facilitates the resolution of complex issues that involve inputs that cannot be compared with one another, typically due to the use of different measurement units. Through the use of AHP, a solution model that employs homogeneous factors is developed from the original problem. To ensure effective comparison of the various parameters, it is crucial that they share common properties, as required by the homogeneity axiom [29]. The method employs pairwise comparisons within a hierarchical structure, with a scale that reflects the degree of dominance of one item over another with respect to a particular attribute [30]. The scale used in AHP is presented in Table 2.

The method involves four key steps: problem definition, determination of priorities, synthesis, and consistency analysis.

To apply AHP in a decision-making process, the first step is to define the goal, which in this case is to choose the most suitable site for photovoltaic (PV) panels. The next stage is to establish a hierarchical structure of the parameters and create a pairwise comparison matrix. For a matrix containing n elements, a total of n(n-1)/2 pairwise comparisons should be made. Superiority is then assigned to the parameter that is at the upper level compared to other parameters according to the scale determined in Table 2.

Table 2
Classification of AHP scales.

Importance	Definition	Explanation
1	Equal	The importance of the parameters are equal
3	Moderate	Slightly favor one parameter over another
5	Strong	Strongly favor one parameter over another
7	Very Strong	Very strongly favor one parameter over another
9	Extreme	Parameter has the highest importance over the other parameter
2,4,6,8	For compromise between the above values	When intermediate values are needed

To ensure consistency in the method, each element of the column is divided by the total of that column, and the row sum of the obtained values is divided by the total number of elements in the row. Additionally, the consistency ratio (CR) test is implemented to validate the pairwise comparisons. In the pairwise comparison stage, if the effect of parameter a on parameter b is 3, the effect of parameter b on parameter a should be 1/3, following the structural axiom. By adhering to this axiom, the CR value will be close to 0, and a CR value below 0.10 indicates that the model is consistent.

The pairwise comparison stage is essential to avoid intuitive behavior in the decision-making process, clarify the decision-making criteria, and calibrate the numerical scale for the measurement of quantitative and qualitative performances [31]. In this study, the parameters used in the site selection for PV in the Menteşe District of Muğla Province are shown in Fig. 2 and elaborated in the following section. It should be noted that, the general criteria of solar energy potential, orography, distance, and environment are well-established and commonly used variables in the literature. However, this study

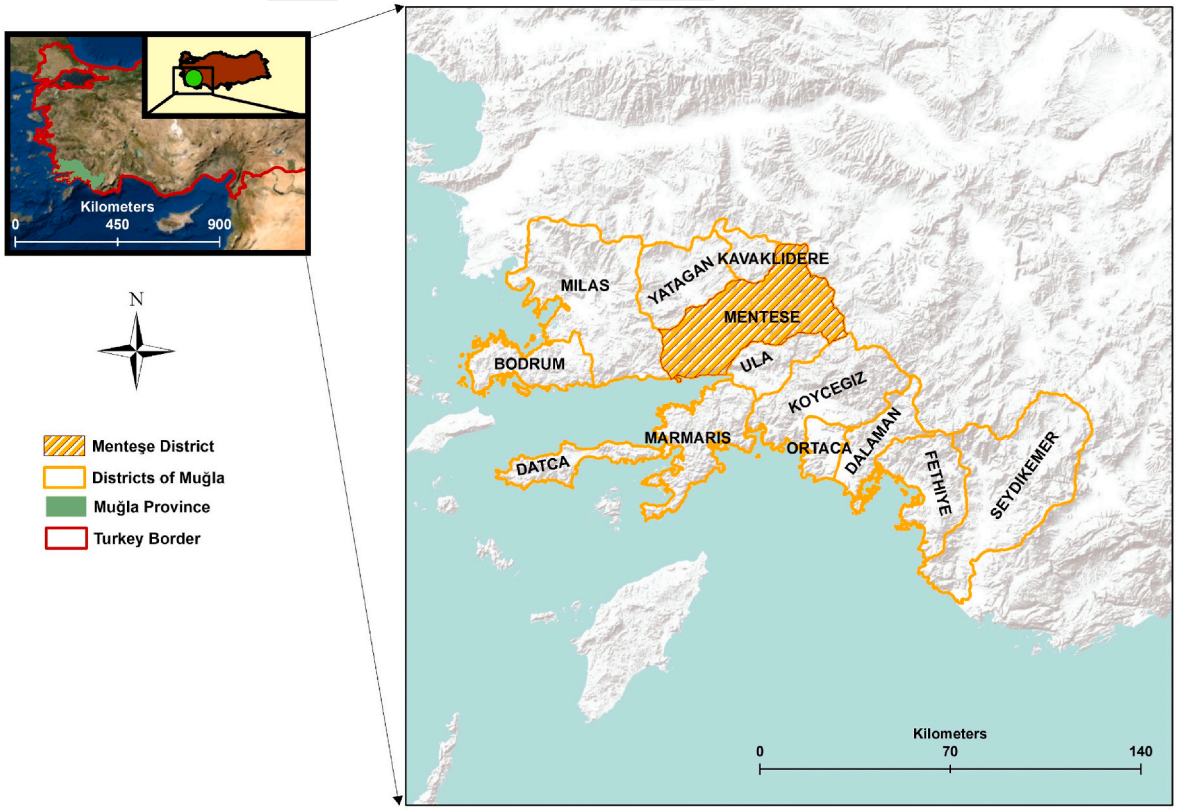

Fig. 1. The geographical location Muğla Province and Menteşe district.

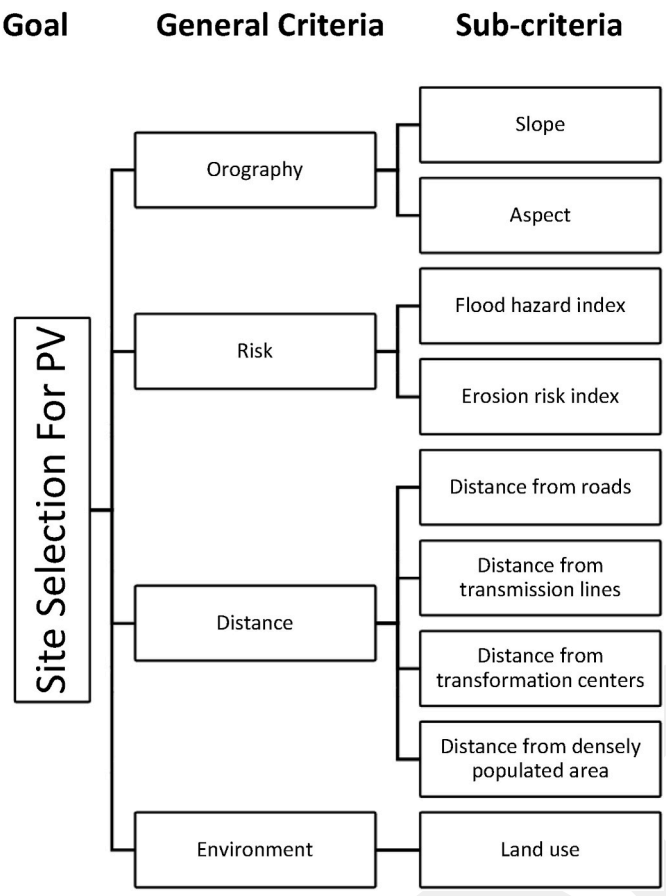

Fig. 2. Goals and criteria for PV site selection.

introduces two novel sub-criteria, namely flood and erosion risk indices, which have not been extensively explored in previous research.

2.3. Criteria determination

According to Miller's psychological experiments [32], the maximum number of comparisons that a person can make without any judgmental errors is 9, so [33] suggested that the number of criteria in the AHP should not exceed 9. In order to ensure the accuracy and reliability of the present study, the number of criteria has been limited to 9, despite the presence of other parameters that may affect the optimal site selection of solar farms. Parameters such as important landscape areas or national parks have been included as buffer zones in the analysis. It is important to note that an eligible PV site should be well irradiated, accessible, and nearly flat while avoiding construction in forests, agricultural, and protected areas. Each variable of the site selection process is explained in the following parts.

2.3.1. Physical solar energy potential

Physical solar energy potential has been identified as the most crucial criterion in numerous studies [16,20]. This criterion consists of temperature and irradiation which can be included as separate parameters as demonstrated in Ref. [25] or if the data is available, they can be combined as solar energy potential as presented in Ref. [21].

Solar energy potential is commonly discussed in terms of two parameters: solar radiation and land surface temperature (LST). The yearly average global horizontal irradiation value of 1300 kWh/m^2 is recommended as the minimum requirement for the area of interest to be eligible for PV construction [34]. Various countries, including Türkiye, have developed their solar radiation maps. As depicted in Fig. 3, Menteşe's solar energy potential is deemed high and adequate for solar PV construction.

Within the Menteşe boundaries, the maximum and average Global Horizontal Irradiance (GHI) values have been identified 1846.70 kWh/m^2 and 1781.43 kWh/m^2, respectively. Areas with lower GHI are primarily situated in valleys with limited sunshine hours due to

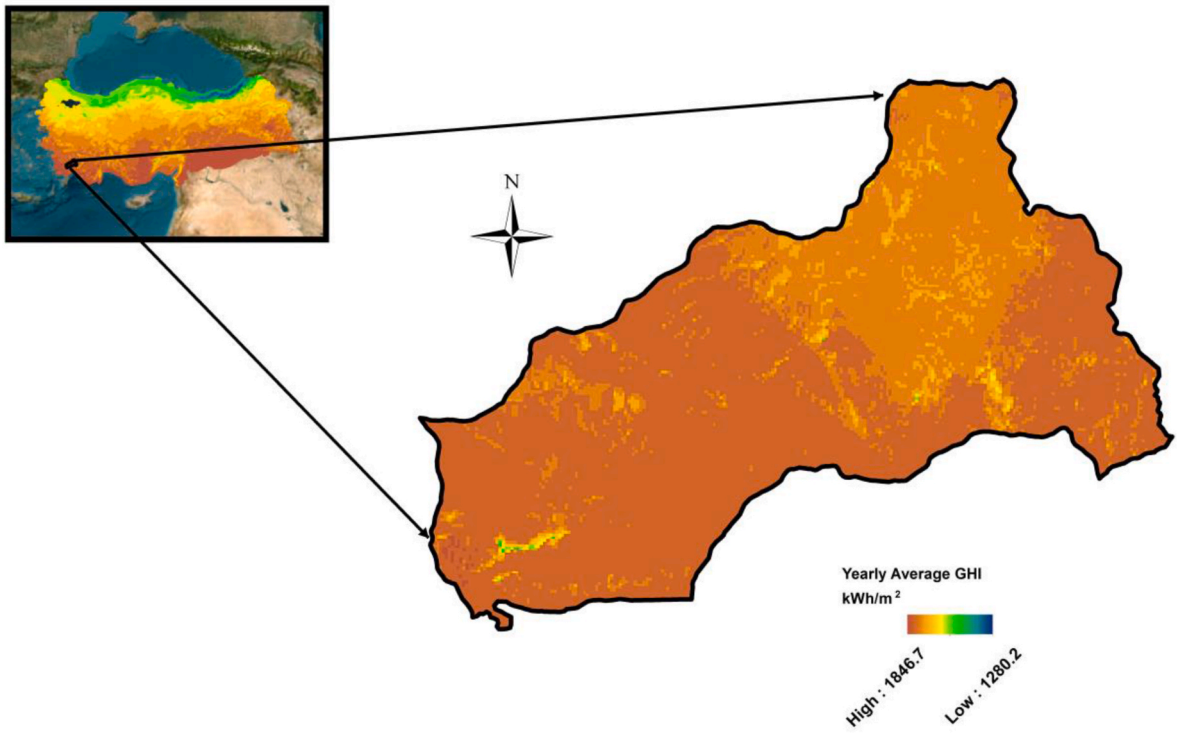

Fig. 3. Spatially varied solar radiation maps of Türkiye and Menteşe district.

topographical features. Nonetheless, these areas are exceedingly small in comparison to the Menteşe's total surface area. GHI values greater than 1500 kWh/m^2 cover an area of 1657.646 km^2, whereas only 1.154 km^2 is covered by GHI values less than 1500 kWh/m^2 but greater than 1280 kWh/m^2. Given the low spatial variability of GHI within the Menteşe District, GHI can be disregarded as a primary variable for the PV site selection process.

2.3.2. Orography and digital elevation model (Slope and aspect)

The investment cost increases when the land is sloped, so flat areas should be preferred in the site selection of PV plants [22,23]. [35] proposed a threshold of the slope for PV plants 3%, whereas the threshold is 5% in Ref. [22]. On the other hand, a much higher threshold was used in Ref. [21] with 20% [9]. preferred to assign a small grade in the AHP when the slope is higher than 10% instead of taking higher slope regions unsuitable.

In order to determine the optimal slope orientations for solar PV construction, the aspect is a crucial parameter that must be taken into account. It is well established that south-facing slopes are the most suitable candidates for this purpose. However, it is important to note that the calculation of slope and aspect within a GIS environment is highly dependent on the topographic resolution of the digital elevation model (DEM). Consequently, the resolution of the DEM has a direct impact on the orography of the study area. To examine this effect, three DEMs with resolutions of 5 m, 25 m, and 34 m were utilized in the calculations, as illustrated in Fig. 4. The 5 m resolution DEM was obtained from the General Directorate of Maps (HGM), the 25 m resolution DEM from COPERNICUS, and the 34 m resolution DEM from SRTM of NASA. As observed in Fig. 4, the minimum and maximum values as well as the spatial variation of the slopes differ among each DEM. This finding is not unexpected, given the lower data quality associated with lower resolutions.

2.3.3. Land use/cover

The determination of land use classes involves the utilization of Sentinel-2 Satellite imagery, which offers a resolution of 9 m. The classification process considers the exclusion of certain land use types, such as croplands, forests, water bodies, and built-up areas, from the available areas for potential solar PV construction. The resulting distribution of land use classes is illustrated in Fig. 5.

2.3.4. Distance

2.3.4.1. Distance from densely populated areas. To reduce transportation costs, PV farms should be located as near as possible to settlement areas [36]. However, PV farms near cities can restrict the growth rate [26], and an optimum distance from cities is necessary to avoid visual intrusion in daylight and noise due to PV farms [7]. To this end, land use data was utilized on the GIS environment to determine the distance from densely populated areas. However, it is important to note that the resultant variable was sensitive to the resolution of the DEM, and thus it was calculated for each resolution in the study.

2.3.4.2. Distance from roads. In the context of site selection studies, roads are often regarded as a crucial factor. The rationale underlying this perspective is to minimize transportation costs while ensuring that construction sites remain accessible. However, most studies typically exclude areas located within a distance of 100 m from roads to prevent potential hazards such as collisions and fires resulting from road accidents. In this study, the vector data of road networks, comprising highways, primary, secondary, and rural roads, as well as their links, were acquired from OpenStreetMap (OSM) data. Subsequently, the vector data of roads were simplified, and orthogonal distances from roads were computed within the GIS environment.

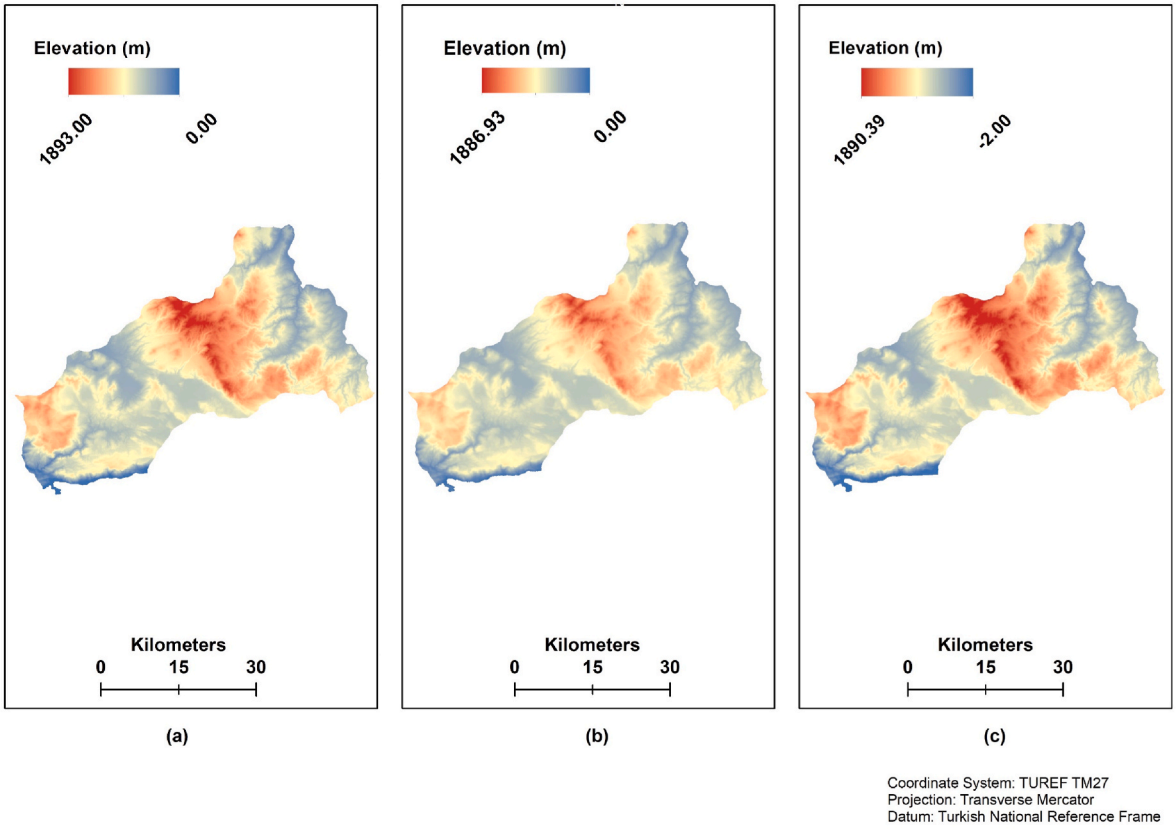

Fig. 4. Digital Elevation Models (DEMs) of Menteşe District with (a) 5 m resolution, (b) 25 m resolution, and (c) 34 m resolution.

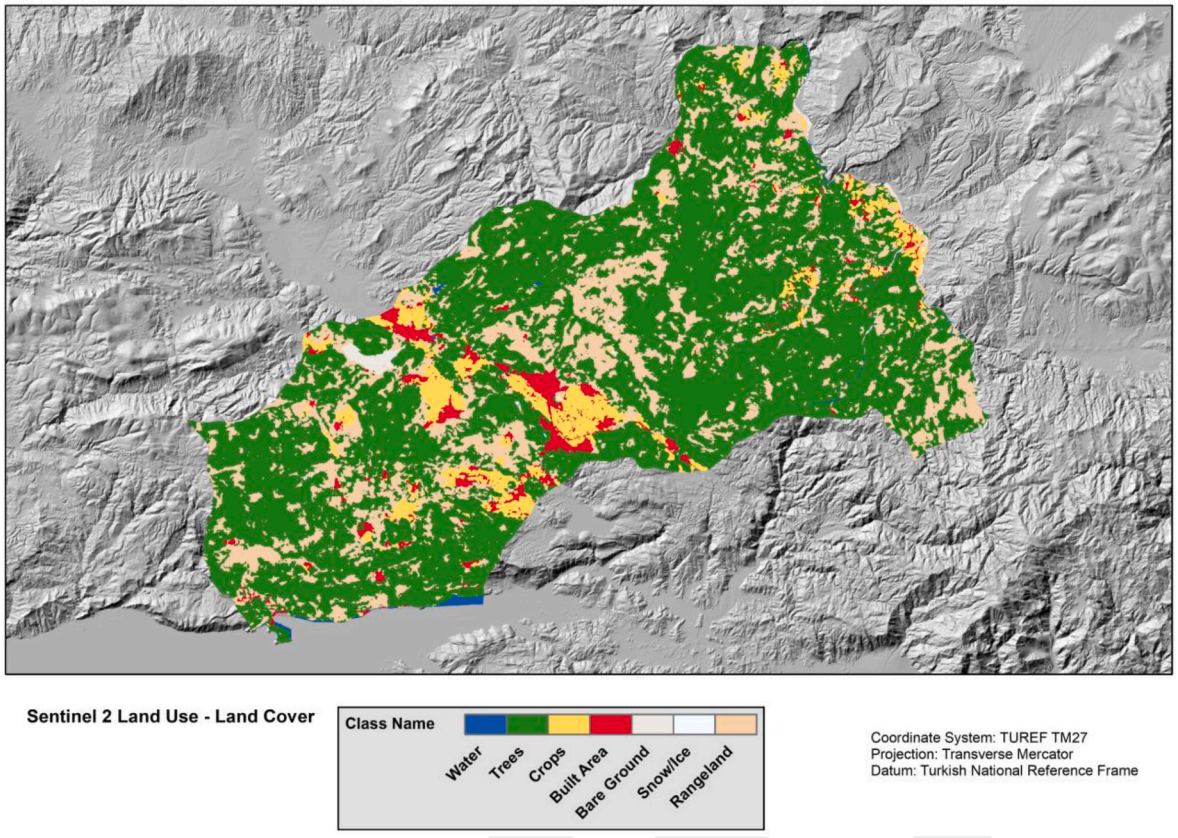

Fig. 5. Land use/land class data of Menteşe district.

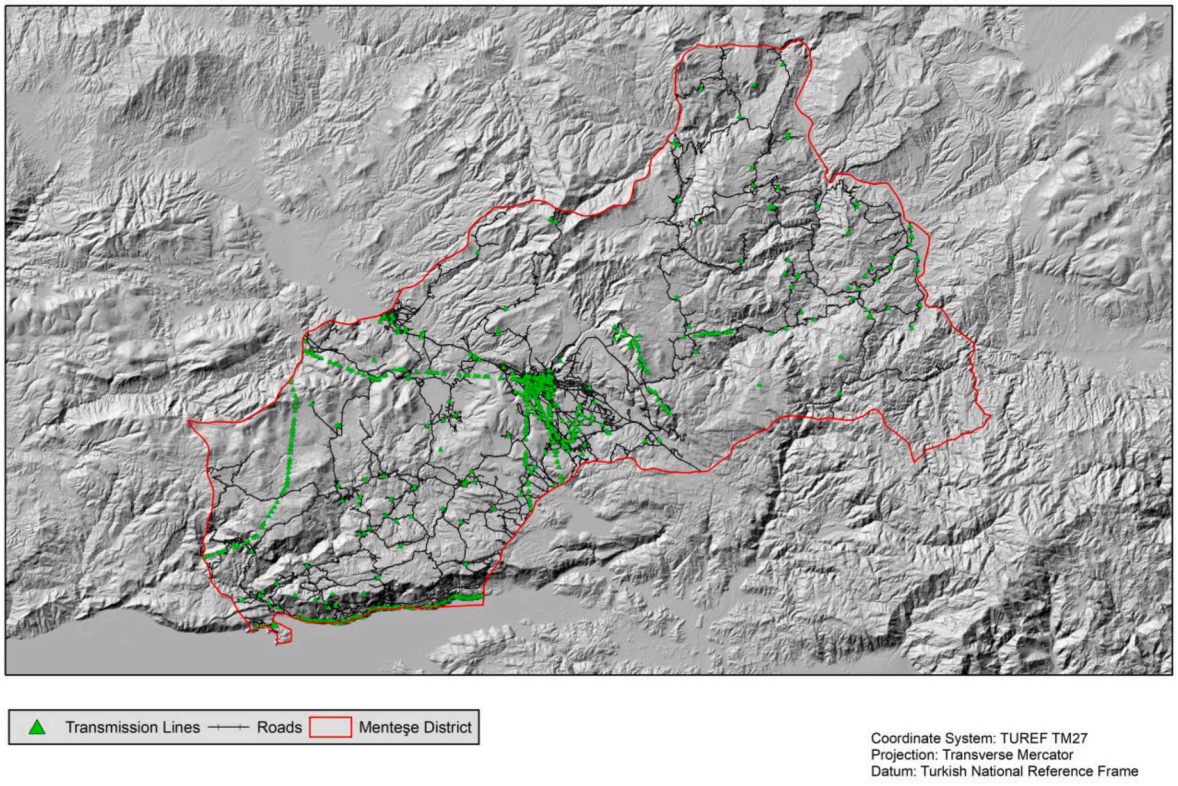

Fig. 6. Roads and transmission lines within the study area.

2.3.4.3. Distance from transmission lines and transformation centers. Transformation centers, which are crucial components of the electricity network, have been identified as a primary variable for PV site selection in several studies. The proximity of PV farms to energy transmission lines and transformation centers is a crucial determinant of the overall cost of construction, as it affects the construction of new energy transmission lines and substations. To account for this, the present study considers the distance from energy transmission lines as a variable in the site selection process, as illustrated in Fig. 6.

2.3.5. Flood hazard index

Floods have been identified as one of the most frequent and destructive natural hazards throughout history, with extreme rainfalls, rapid urbanization, changing climate, and global warming as the leading causes [37,38]. Predictably, floods are expected to become more frequent and devastating in the upcoming decades [39]. Moreover, breaching of dams also causes extreme flooding, especially in the area located at the downstream of a dam. There are various studies that examine the potential hazards related to dam break, and behavior of a structure when it is in contact with the fluid [40–43]. Therefore, PVs can suffer from structural failure or deformation in case of a dam failure or flooding.

In light of this, the present study considers river and dam breach related floods as the primary variable for optimal site selection of PVs. However, previous studies have suggested arbitrary exclusion zones, with [21] recommending a 100 m exclusion zone from dams and disregarding river floods, while [16] suggest a 5 km distance from dams to avoid flood-related damage to the PVs.

To overcome these limitations, the present study proposes a novel approach to determine exclusion zones related to rivers and dams through a concrete methodology. Specifically, a flood risk index is determined through hydraulic modelling to quantify the related flood hazard, utilizing spatially varied flow depth and flood propagation velocities of the Menteşe District. Furthermore, hydraulic modelling was employed to determine flow depth and velocities in case of a failure of Bayır Dam, which is located within the Menteşe District Boundary. A detailed description of the proposed methodology is presented below.

2.3.5.1. The failure of Bayır Dam. The hydraulic modeling for the potential failure of Bayır Dam was conducted using the most severe dam breach scenario, which is the overtopping of the dam crest. To predict essential parameters associated with the dam breach, including breach time, breach slope, and final breach width, the equations proposed by Ref. [44] were utilized.

$$B_{ave} = 0.27 K_0 V_w^{0.32} h_b^{0.04} \quad (1)$$

$$t_f = 63.2\sqrt{\frac{V_w}{g h_{b_w}^2}} \quad \text{for easily erodible} \quad (2)$$

where B_{ave} is the average breach width (in meters), K_0 is the failure mode constant (1.3 for overtopping and 1.0 for piping), V_w is the reservoir volume at the time of failure (in cubic meters), h_b is the height of the final breach (in meters), g is the gravitational acceleration (in meters per second squared), and t_f is the time of breach formation (in seconds).

The hydraulic modeling of dam breach was conducted through a two-phase approach. In the first phase, a one-dimensional dam breach model was constructed, and as a result of the hydraulic model, the breach hydrograph presented in Fig. 7 was obtained.

In the second phase of the study, the terrain was generated by implementing a 5 m resolution DEM, and the one-dimensional (1D) breach hydrograph was utilized as a boundary condition for the two-dimensional (2D) hydraulic model. The building data of the study area was generated by considering the Airbus Satellite View data. As a result

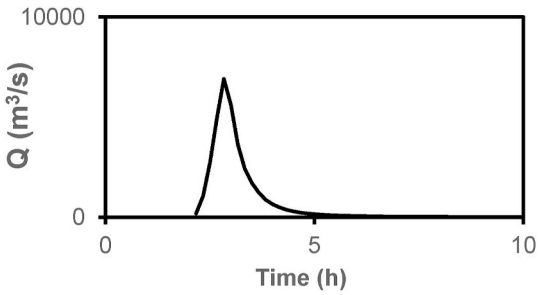

Fig. 7. Dam Breach Hydrograph for the case of Overtopping.

of this approach, the inundation area and corresponding flow depths and flood propagation velocities that could arise due to the potential dam breach were obtained. These results are depicted in Figs. 8a and 9a.

2.3.5.2. River flood case. Within the boundaries of the Menteşe District, a complex network of rivers is present, which poses a significant risk of flooding. To assess this risk, the results of the Western Mediterranean Basin Flood Management Plan were consulted, and the resulting flow depths and flood propagation velocities, obtained from the flood management plans of General Directorate of Water Management, are presented in Figs. 8b and 9b.

2.3.5.3. Hazard assessment. The proposed methodology for incorporating the flood risk index as a variable for site selection entails a systematic quantification of flood hazards, which involves linking hydraulic models of urban floods and dam breaches with the process of solar PV site selection. Numerous approaches for flood hazard quantification have been documented in the literature. [54] introduced a popular and established method for the quantitative assessment of flood hazard, and the corresponding flood hazard thresholds and vulnerability curves are depicted in Fig. 10.

[45] have suggested that H6 hazard class-prone areas are susceptible to structural failure, even when the flow is non-Newtonian [45]. Thus, solar PVs should not be sited in areas prone to H4–H5 and H6 hazards. Following the implementation of the hydraulic model for dam breach, the flow depth and flood propagation velocities were determined, and the hazard classes for the study area were calculated and presented in Fig. 11. As mentioned earlier, the primary goal of hydraulic modeling and corresponding hazard classes is to establish a robust methodology for determining exclusion zones from dams, rivers, lakes, etc. in the PV site selection process. The hazard class outcomes presented in Fig. 11 reveal that while solar PVs can be positioned 100 m from the dam as proposed in previous studies, at 5.5 km downstream of the dam, an H6 class hazard exists that could lead to structural failure. Consequently, the implementation of spatially varied hazard classes as variables for PV site selection is advantageous.

2.3.6. Erosion risk index

Erosion is a natural hazard that poses a significant risk to the structural integrity of various installations, including solar photovoltaic (PV) systems. It is worth noting that both wind and water contribute to erosion. According to the State Planning Organization (DPT) of Türkiye [56], water and rainfall account for 99% of erosion in the country, while wind contributes to the remaining 1%. In the present study, the erosion risk was considered the primary factor for the optimal site selection of PVs, as it can seriously undermine their structural stability.

Various methods have been proposed in the literature to quantify erosion or estimate the annual soil loss caused by water or rainfall. The Universal Soil Loss Equation (USLE) [46] and the Revised Universal Soil Loss Equation (RUSLE) [47] are two widely accepted and commonly used approaches. The RUSLE method considers several primary factors that influence erosion, including rainfall-erosivity, soil sensitivity to

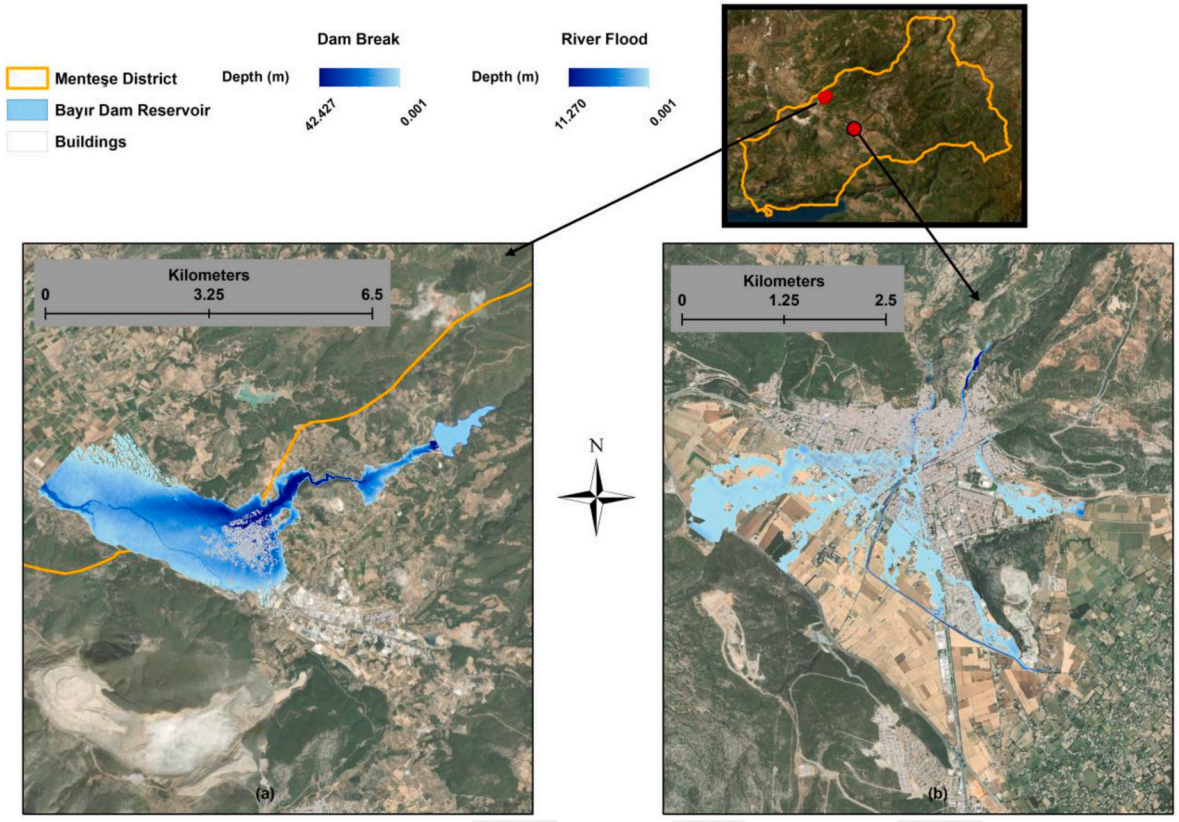

Fig. 8. Flow depths of (a) dam break and (b) river flood.

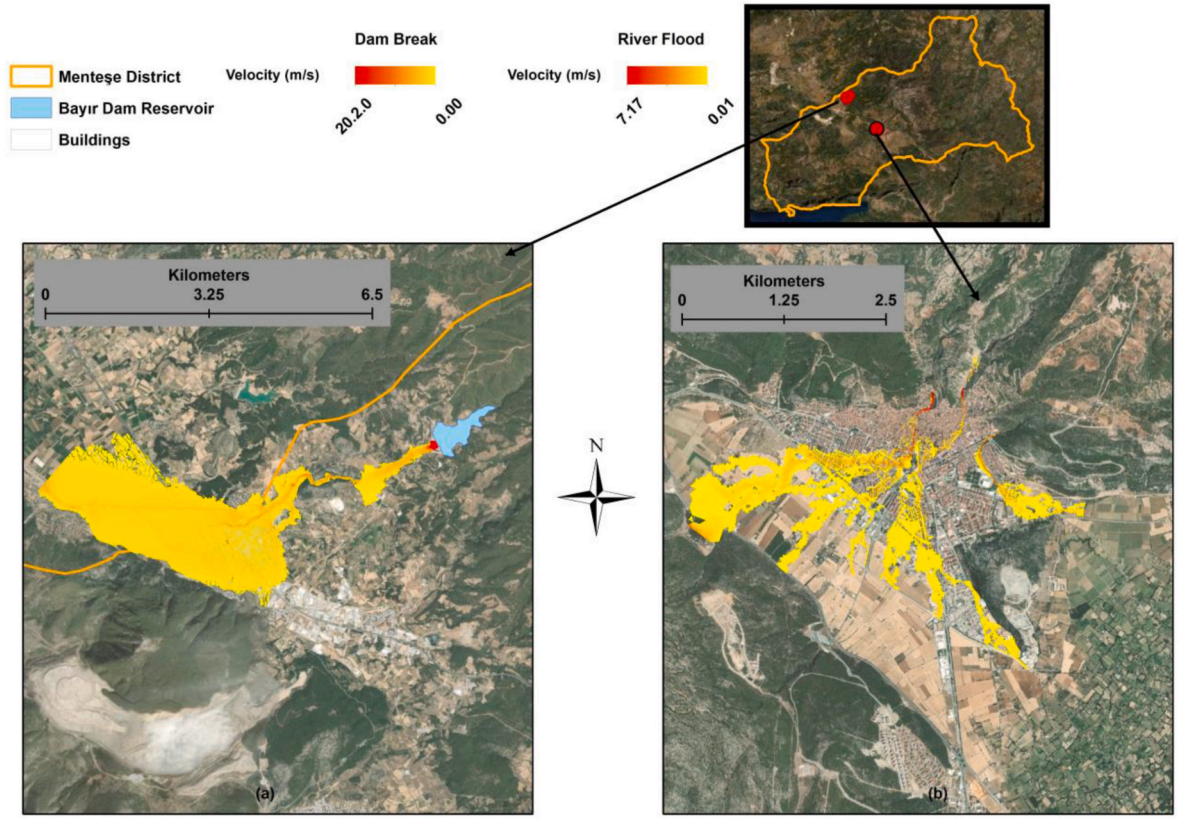

Fig. 9. Flood propagation velocities of (a) dam break and (b) river flood.

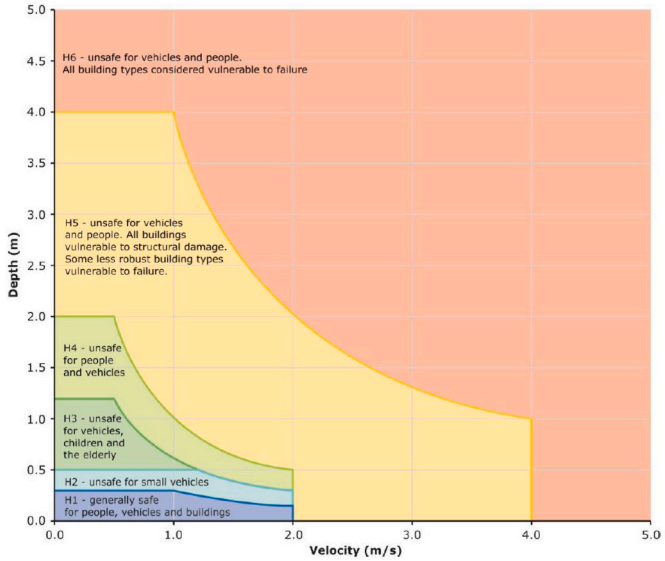

Fig. 10. Flood Hazard Classes [54].

erosion, topographic features such as slope length and steepness, and crop management and support practices. The RUSLE equation is given as follows:

$$A = R\ x\ K\ x\ LS\ x\ C\ x\ P \tag{3}$$

where A is annual soil loss (t/ha/yr), R is rainfall-runoff erosivity factor, (MJ/mm/ha/h/yr), K is soil erosion sensitivity factor, L is slope length factor, S is slope steepness factor, C is cover management factor and P is the support practices factor.

The R and K values of the RUSLE were determined and calibrated throughout Europe, including Türkiye, by the study of [48]. Thus, the R and K values for the project area were derived from the data of the aforementioned study [48]. The LS factor of the study area was calculated based on a 5-m resolution DEM on the GIS environment. To perform the LS calculations, the equation proposed by Ref. [49] was implemented. The cover management and support practices factors were calculated on the GIS environment by taking into account the land use classes and constraints acquired from the literature [50,51]. The spatially varying RUSLE parameters and the corresponding erosion and annual soil losses are presented in Fig. 12.

To translate the erosion results into actionable insights for site selection, the severity of erosion is categorized into different classes using the erosion severity classes suggested by the USDA, which are presented in Table 3 [52]. The severity classes were then used to identify exclusion zones for the solar PVs. Based on the erosion severity analysis, areas with "severe" and "very severe" erosion were classified as exclusion zones.

2.4. Priorities among criteria with AHP

Since the AHP minimizes the cognitive errors and can make a comparison of both qualitative and quantitative parameters, it has been widely applied to many different areas. However, defining the priorities in the AHP is a tedious task. In the problem of determining the suitable locations of solar farms, various criteria should be classified and prioritize among each other. Studies in the related literature have shown that different number of criteria can be defined. In addition, final weights of the criteria calculated from the AHP change considerably in different studies, although consistency ratio of the AHP suggests that the weights are consistent. To prevent a bias, the weights calculated from the AHP considering previous studies and expert opinions are compared with a method assigning weights using a ranking and nonhierarchic comparison proposed in Ref. [53]. The final weights calculated from the AHP

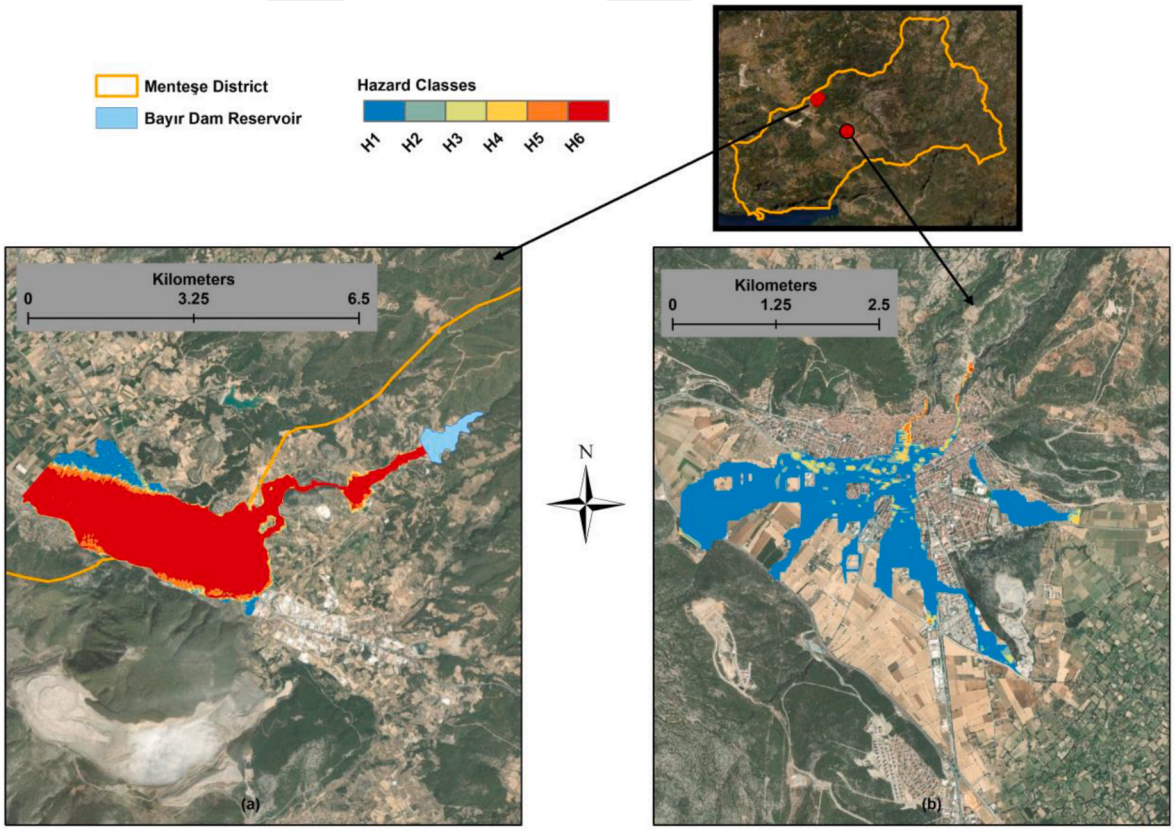

Fig. 11. Spatially varied hazard classes of (a) dam break and (b) river flood.

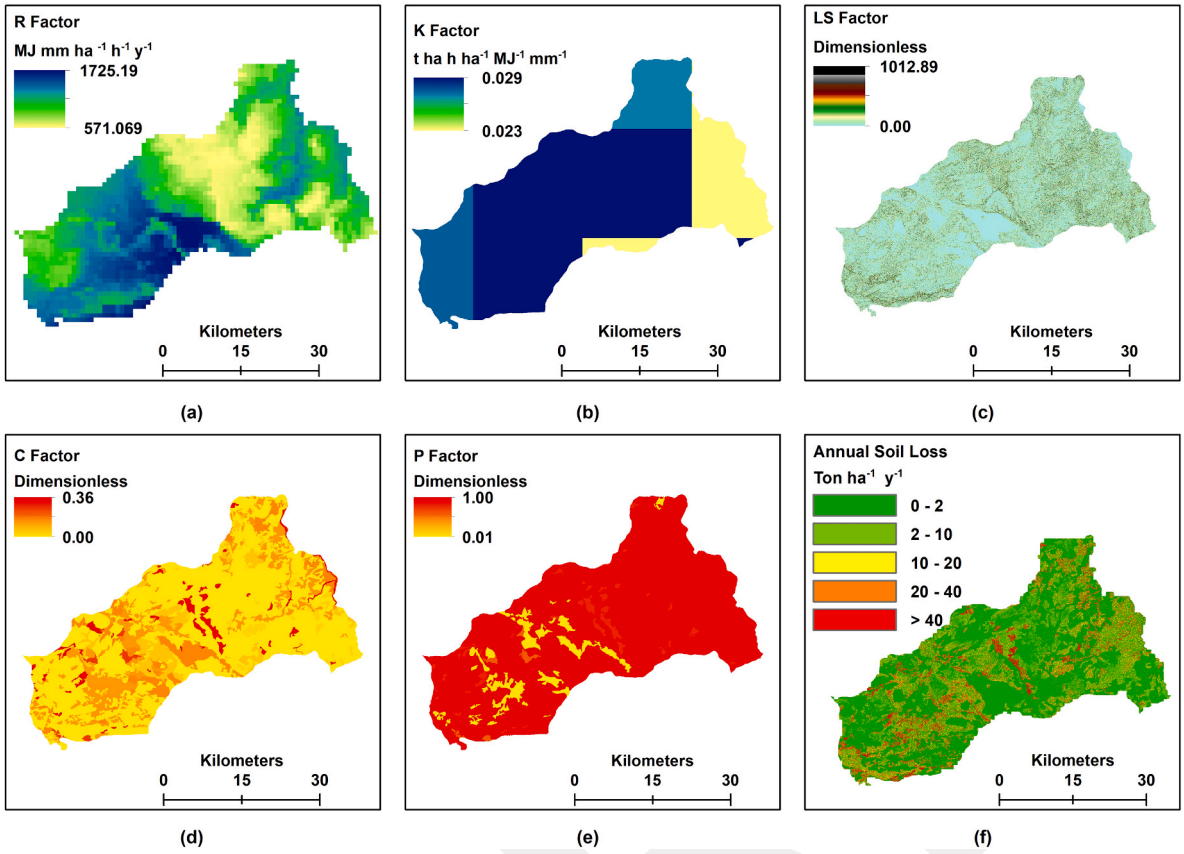

Fig. 12. Spatially varied RUSLE parameter (a-b-c-d-e) and Annual Soil Loss (f).

Table 3
Erosion severity classes.

Erosion (ton/ha/year)	Erosion Class
0–2	Very Slight
2–10	Slight
10–20	Moderate
20–40	Severe
>40	Very Severe

Table 4
Factor Weights for solar PV installation.

Criterion	Weights of		Difference (%)	Weights of AHP – without considering natural hazards (%)
	AHP (%)	The method in [53]		
Slope	19.02	20.26	6.53	24.51
Aspect	16.99	17.59	3.52	20.80
Distance from transmission lines	15.78	15.04	4.69	18.95
Distance from densely populated area	13.56	13.83	1.99	17.03
Flood hazard index	9.32	9.12	2.14	–
Erosion risk index	8.79	8.06	8.31	–
Land Use/Cover	6.80	7.03	3.26	7.62
Distance from roads	5.37	5.01	6.61	6.07
Distance from transformation centers	4.36	4.05	7.04	5.02

and the method of [53] is given in Table 4. The maximum difference between AHP and the method in Ref. [53] is observed in erosion risk index with 8.31%. The minimum difference is in distance from densely populated area with 1.99%. It should be noted that relative priorities of different parameters are defined rather subjectively in both AHP and the method in Ref. [53], although expert opinions and the studies in the literature are considered. Therefore, the difference between two methods is considered to be acceptable. In addition, the consistency ratio is calculated as 0.011 which is way less than the threshold value 0.1, so the procedure of AHP is accurate.

The weights are also determined without considering natural hazards which are flood risk and erosion as can be seen in Table 4. For that case the consistency ratio is found to be 0.016 also way less than the threshold value of 0.1. The main and sub-criteria and the corresponding weights and indicators used in the implementation of criteria used in AHP into GIS environment are shown in Table 5.

2.5. Scenarios

To incorporate the effects of flood hazard and erosion risk in the site selection process for solar PVs, two scenarios were developed using the 5 m resolution DEM. The first scenario utilized seven criteria, namely slope, aspect, distance from transmission lines, distance from densely populated areas, land use/cover, distance from roads, and distance from transformation centers. The second scenario included flood hazard and erosion risk indices as additional criteria, thereby expanding the list of factors used in site selection.

It should be noted that, the sub-variables of distance and orography are directly related to the topographic resolution. Thus, to evaluate the impact of topographic resolution on solar PV site selection, these sub-variables, considered in Scenario 2, were recalculated for DEMs with resolutions of 25 m and 34 m and they are included in Scenario 3 and

Table 5
Factor weights with assigned grades for solar PV installation.

Criterion	Weight	Sub-criteria	Indicators	Criteria	Weight	Sub-criteria	Indicators
Slope (%)	19.02	0–2	9	Erosion risk index	8.79	0–2	9
		2–5	6			2–10	7
		5–10	2			10–20	4
		10–20	1			20–40	0
		>20	0			>40	0
Aspect	16.99	East	2	Land Use/Cover	6.80	Bareground	9
		West	2			Rangeland	9
		South	9			Water body	0
		North	1			Forest	0
		southeast	6			Cropland	0
		southwest	6			Built area	0
		northeast	1			Mine site	0
		northwest	1				
Distance from transmission lines (km)	15.78	0–1	9	Distance from roads (km)	5.37	0–0.1	0
		1–2	8			0.1–1	9
		2–4	6			1–2	8
		4–8	3			2–4	6
		>8	0			4–8	3
						>8	0
Distance from densely populated area (km)	13.56	0–1	0	Distance from transformation centers (km)	4.36	0–1	9
		1–5	9			1–5	8
		5–10	6			5–10	7
		10–20	4			10–20	5
		>20	2			>20	3
Flood hazard index	9.32	No risk	9				
		H1	8				
		H2	7				
		H3	5				
		H4	1				
		H5	0				
		H6	0				

Table 6
Scenarios for PV site selection.

Criterion	Scenario 1 (Sc-1)	Scenario 2 (Sc-2)	Scenario 3 (Sc-3)	Scenario 4 (Sc-4)
DEM	5 m	5 m	25 m	34 m
Slope	x	x	x	x
Aspect	x	x	x	x
Distance from transmission lines	x	x	x	x
Distance from densely populated area	x	x	x	x
Flood hazard index	–	x	x	x
Erosion risk index	–	x	x	x
Land Use/Cover	x	x	x	x
Distance from roads	x	x	x	x
Distance from transformation centers	x	x	x	x

Scenario 4, respectively. The summary of these scenarios is provided in Table 6.

3. Results and discussion

3.1. The effect of flood and erosion risk indices on PV site selection

Fig. 13 presents the optimal locations for solar PVs, specifically determined for Sc-1 and Sc-2. The figure reveals that densely populated areas are deemed unsuitable for the construction of solar PVs as can be seen in the restricted indicators (shown with 0) in Table 5. This aspect is crucial as it also eliminates the risk of river flooding in the study area, given that major rivers are predominantly situated in densely populated regions.

The suitability for constructing PVs varies based on the flood and erosion risk indices, leading to differences in the total eligible area. For an in-depth analysis, the suitable zones for Sc-1 and Sc-2 are presented in Table 7, providing an overview of the total area of eligible sites. The total suitable area is 132.40 km^2 for Sc-1 and 124.99 km^2 for Sc-2. The notable difference in the total area of suitable zones between Sc-1 and Sc-2 can be attributed to the introduction of flood and erosion indices, despite their relatively lower weights in the AHP. Since the criteria causing restrictions are the same in both Sc-1 and Sc-2, except for the inclusion of flood and erosion indices, this difference is noteworthy. Sc-2, which takes into account flood hazard and erosion risk, has a smaller total area of eligible sites compared to Sc-1. This indicates that the presence of these factors decreases the number of suitable zones for PV panel installation. In contrast, Sc-1, which does not consider flood hazard and erosion risk, has a larger area categorized as suitable for PV panel installation. However, it should be noted that in Sc-2, although the total suitable area is less, there are higher proportions of moderately and extremely suitable zones. This difference can be explained by the nature of the AHP. As shown in Table 4, since the weights of flood and erosion indices are not included in Sc-1, the weights of other criteria increase, leading to an increase in the moderately and extremely suitable areas. However, the overall suitable area decreases due to the emergence of new restricted zones identified by the flood and erosion indices as expected.

Previous case studies have indicated varying levels of suitability for PV site selection [9]. reported a suitability of approximately 60% in Karapınar, while [16] found a suitability of approximately 85% for PV installation in Morocco. In a study conducted by Ref. [19] in Murcia, the total suitable site was determined to be 13.85%.

In the current study, the findings reveal that approximately 7.5% (124.99 km^2) of the total area (approximately 1659 km^2) is eligible for the construction of solar PV panels. This discrepancy in suitability can mainly be attributed to the topography of the selected area. The chosen region exhibits a higher proportion of mountainous terrain, resulting in steeper slopes and an abundance of forests due to the Mediterranean climate. In contrast, the study areas investigated by Refs. [9,16] had different topographical features including a higher proportion of flat regions.

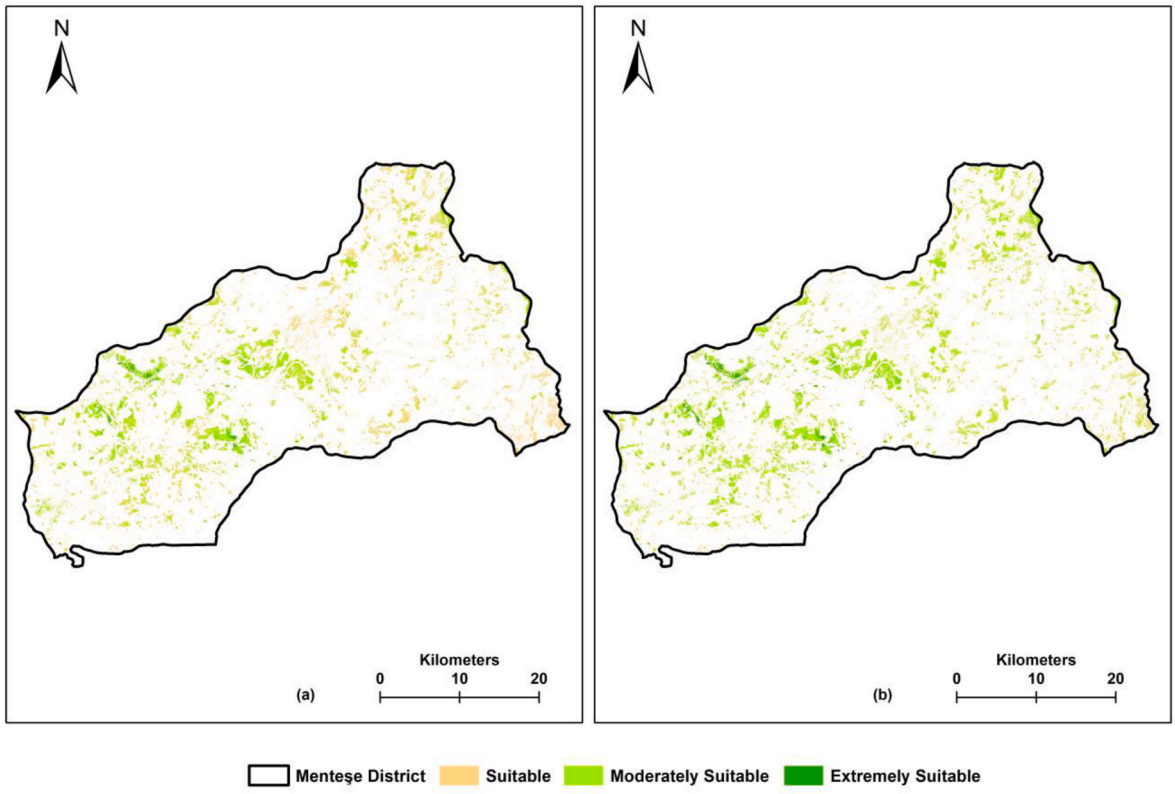

Fig. 13. Optimal Location for solar PVs (a) Sc-1 and (b) Sc-2.

Table 7
Total area of suitable zones.

Suitability	Sc-1 Area (km^2)	Sc-2 Area (km^2)
Suitable	48.76	13.27
Moderately Suitable	76.18	100.94
Extremely Suitable	7.47	10.78
Total Eligible Area	132.40	124.99

Although the percentage of eligible sites in this study is comparable to that reported by Ref. [19]; the inclusion of erosion and flood indices reduces the number of suitable zones for solar PV construction.

Fig. 14 provides a detailed analysis of areas vulnerable to flood hazards resulting from dam breaks and areas susceptible to erosion risks. In the figure, eligible areas for Sc-1 are represented by blue color, while eligible areas for Sc-2 are depicted in yellow.

The results demonstrate that the occurrence of dam breach flood hazards influences the selection of optimal PV sites. Notably, certain zones along the dam axis are eliminated as unsuitable. Furthermore, despite being approximately 1.5–5.5 km away from the dam body, a blue-colored region shown in Fig. 14b measuring 0.2 km^2 is also excluded due to dam break-related hazards.

Moreover, smaller areas depicted in blue in Fig. 14a and (c) are eliminated due to the presence of erosion risk indices. The influence of erosion and flood risks on site suitability is also summarized in Table 7. These findings suggest that the erosion and flood risk should be carefully considered when selecting the optimal location for the solar PVs.

3.2. The effect of topographic resolution on PV site selection

In order to assess the impact of topographic resolution, DEMs with varying resolutions of 5 m, 25 m, and 34 m were considered. The AHP methodology used in Sc-2, which accounts for both flood and erosion risks, was reapplied to the 25 m and 34 m resolution DEMs, resulting in Sc-3 and Sc-4, respectively. A comparative analysis of Sc-2, Sc-3, and Sc-4 is presented in Fig. 15 to evaluate the influence of topographic resolution on solar PV site selection.

It is noteworthy that the calculation process involved in determining the distance to roads, transmission lines, and other factors requires the use of digital elevation models (DEMs). Therefore, variables such as distance from roads, distance from transformation centers of Sc-3 and Sc-4 are affected by DEMs resolution. As a result of lowering DEM resolution, there may be optimal sites identified in forested areas, urban regions, or even within dam reservoirs.

Fig. 15 indicates that the implementation of Sc-3 and Sc-4 or DEMs with 25 m and 34 m resolution provides an area that is approximately the same. While there may be some voids or negligible shifts, the results are generally satisfactory. However, there is a shift in the optimal sites that can result in optimal sites being identified in areas such as trees, water bodies, or croplands in land use classes. The main reason for this situation is the difference in resolutions between the land use data and the DEM. As previously mentioned, land use data has a resolution of 9 m, which means that 1 attribute such as tree or cropland is assigned to a 9 m × 9 m area. On the other hand, if a DEM has a resolution of 25 m, this means that a 25 m × 25 m square has an elevation attribute. Additionally, calculations for slopes, aspect, and distance are carried out for the specified resolutions. Consequently, the difference in resolution between the DEM and land use data can result in inconsistencies. Therefore, it is suggested that when implementing the site selection procedure using AHP, the resolution of the DEM should be equal to or smaller than the resolution of the land use data. It is important to note that the site selection process in a GIS environment typically relies on topographic data for calculating distances, slope, and other factors. However, many studies [9,16,20] do not provide precise information about the resolution of the data. While some studies [21,36] provided clear information about the resolutions of the data used, they did not delve into the discussion of the effect of these resolutions. In this study, for the first time in the literature, the effect of different DEM resolutions

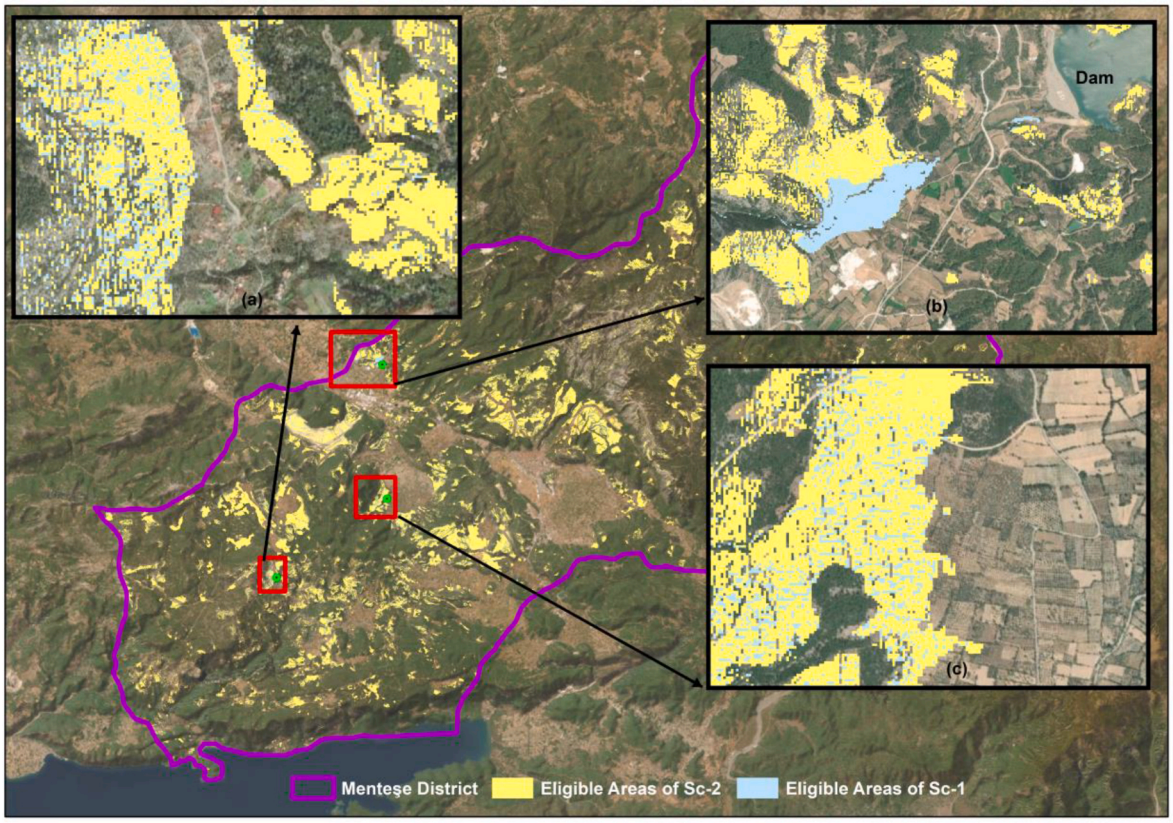

Fig. 14. The comparison between optimal PV sites determined from Sc-1 and Sc-2.

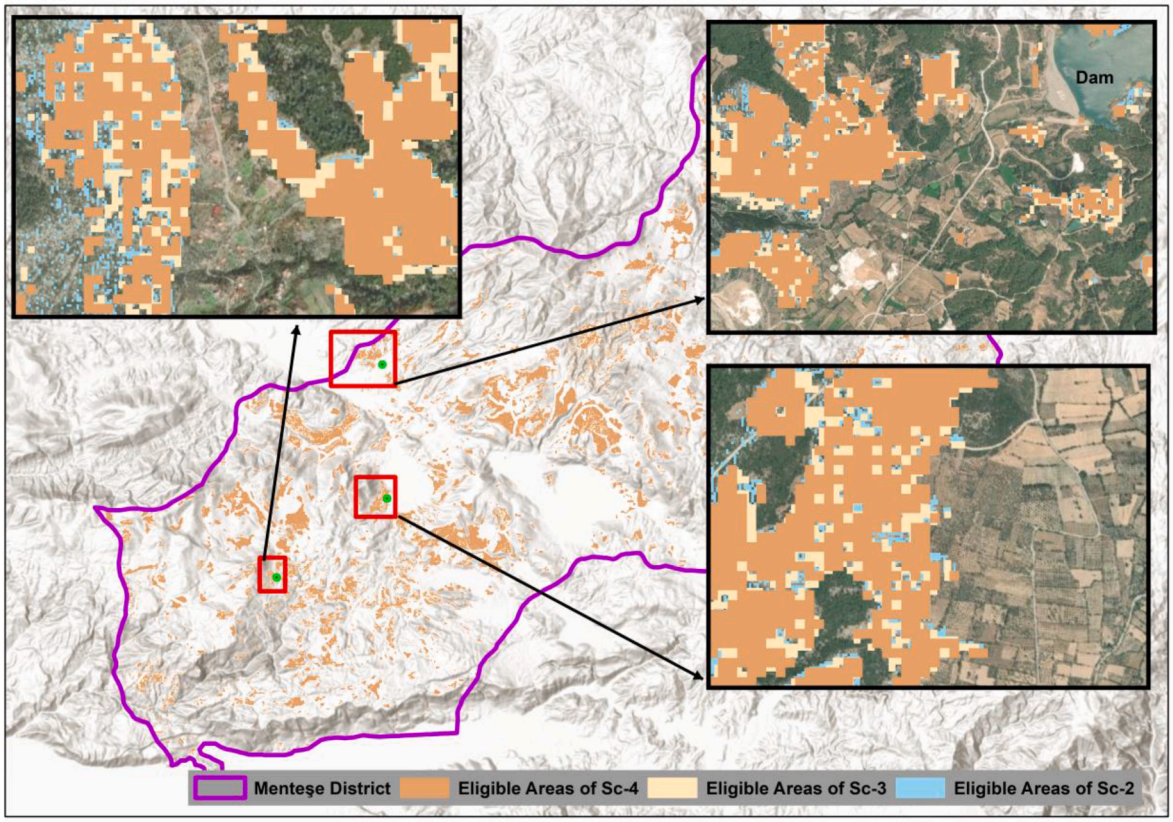

Fig. 15. Effect of topographic resolution on optimum site selection.

on the identification of suitable sites for PV construction was investigated.

3.3. Comparison of suitable locations with the existing solar farms

The analysis of previous PV farms and their comparison with Sc-1 and Sc-2 demonstrates the accuracy of the predictions. It is observed that the existing PV farms are primarily located in flat areas, particularly in rangelands and bare lands. Nevertheless, it is crucial to bear in mind that the construction of PVs must take into account not only technical feasibility but also economic considerations. In some instances, buyout/acquisition costs can become prohibitively high, making cost-benefit analyses impractical. However, technical feasibility studies can provide valuable insights into eligible areas that are free from risk and offer maximum efficiency. Furthermore, PV panel construction sites are often chosen by considering land owned by the state. A comparison of Sc-1 and Sc-2 with existing PV farms is presented in Fig. 16.

It is observed that in certain cases, the areas predicted in Sc-1 and Sc-2 do not align with the existing PV farms. The primary reason for this deviation is the road constraint present within both Sc-1 and Sc-2.

Polygons 1, 2, and 4, which represent existing farms, are located within the eligible sites for both Sc-1 and Sc-2. However, PVs represented by Polygon-3 and a section of PVs enclosed by Polygon 5 are not situated within the eligible sites for either Sc-1 or Sc-2. This discrepancy is caused by the "distance to roads" constraint, as depicted on the map.

Furthermore, it should be noted that the hillshaded map indicates that both existing PVs are positioned on flat surfaces within highly elevated regions, away from populated areas. This strategic placement helps to safeguard the existing PVs from erosion-prone areas and potential flood hazards associated with dam-break scenarios.

The primary variables of site selection for PVs include solar potential, land use, orography, and distance. Existing studies in the literature often define resolution as either high or sufficient without providing precise details about the resolution and its impact. Additionally, the literature lacks clear specifications regarding the resolution, land use, and orography. However, this study demonstrates that the resolution of topography and land use significantly affect the identification of suitable sites. Furthermore, the inclusion of new variables such as flood and erosion risk indices are crucial and cannot be overlooked in the site selection process based on the fact that climate change-driven hydrological extremes are inevitable. Moreover, in most studies, solar potential is considered as a primary variable when selecting sites. However, in this study, solar potential is not included as a variable due to its uniform distribution across the study area. An examination of the optimal sites of each scenario reveals that the site selection process necessitates a site-specific and multidisciplinary approach. Instead of considering variables that are frequently mentioned in the literature, different variables should be included regarding the unique characteristics of the area.

4. Conclusions

The increasing need for renewable energy sources has led to a growing interest in the use of solar panels as an efficient and sustainable energy-generating technology. While many studies have been conducted to determine the optimum location of PV panels, most of them utilize the same procedure with the same variables for different zones. This study, on the other hand, emphasizes the consideration of flood and erosion risk as criteria for site selection, and evaluates various topographic resolutions to assess their effect on PV site selection. The results demonstrate that flood and erosion risk have a non-ignorable impact on the site selection process, leading to changes in suitability and a decrease in the total area of eligible sites, despite their relatively lower weights in the AHP. Furthermore, it is important to highlight that unlike previous studies that consider flood risk based on a fixed distance from dam bodies, this study reveals that determining a constant distance from dams lacks a scientific basis. As depicted in the study, there are areas

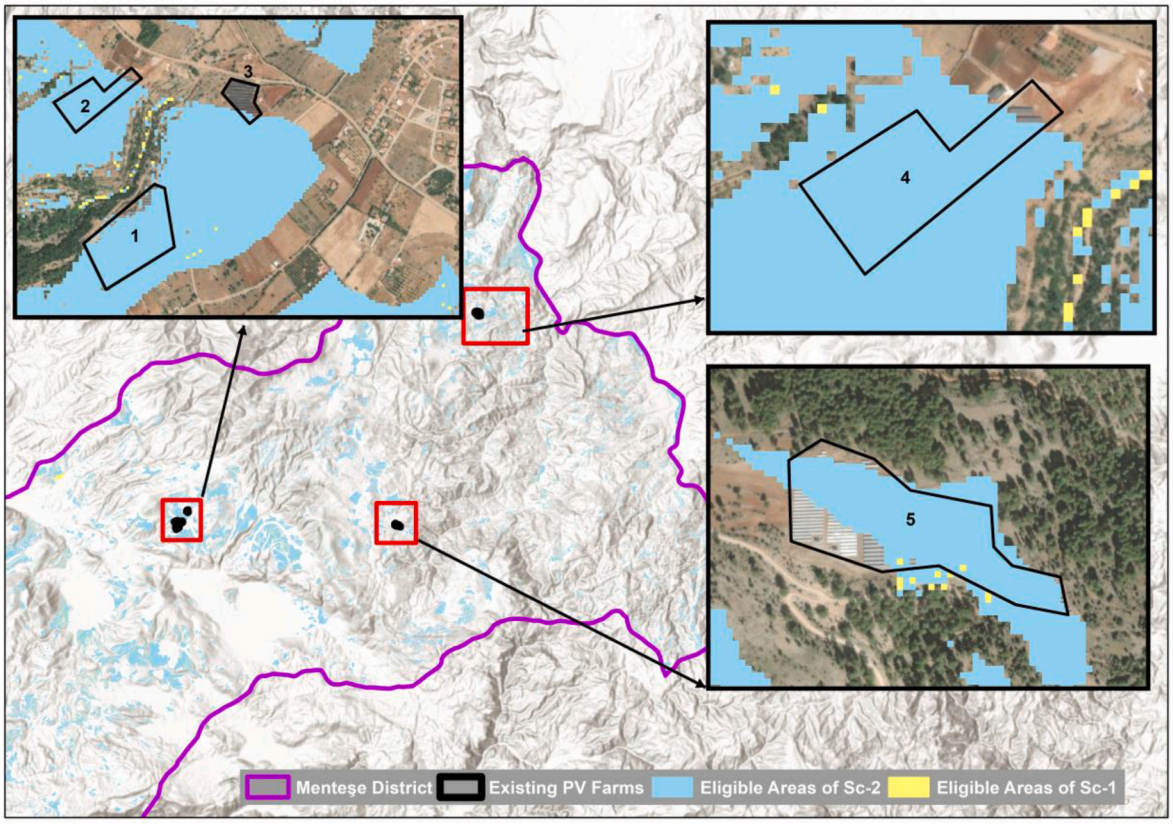

Fig. 16. Evaluation of existing PV farms with Sc-1 and Sc-2.

located 5.5 km away from the dam body that remain under the risk of dam-break-related hazards and are thus ineligible sites for PV panel installation. Additionally, the study demonstrates that low-resolution topographic data can be used for site selection, provided that the data is resampled to the resolution of land use data.

In summary, this study highlights the importance of adopting a multi-disciplinary approach in the site selection of PV panels regarding the physical characteristics of the study area. By incorporating flood and erosion risk indices, the need to evaluate potential variables beyond the existing literature is emphasized. This holistic approach ensures a more accurate and effective selection of eligible areas for PV panel installation, considering factors crucial for their long-term viability and sustainability.

CRediT authorship contribution statement

Kutay Yılmaz: Conceptualization, Methodology, Formal analysis, Investigation, Writing – original draft, Visualization. **Ali Ersin Dinçer:** Conceptualization, Methodology, Investigation, Writing – original draft, Writing – review & editing. **Elif N. Ayhan:** Writing – original draft.

Declaration of competing interest

The authors declare that they have no known competing financial interests or personal relationships that could have appeared to influence the work reported in this paper.

References

[1] IEA, World Energy Balances [WWW Document], World energy balances, 2022. URL, https://www.iea.org/data-and-statistics/data-product/world-energy-balances, 11.8.22.

[2] P. Kaiser, B. Unde, C. Kern, A. Jess, Production of liquid hydrocarbons with CO2 as carbon source based on reverse water-gas shift and fischer-tropsch synthesis. https://doi.org/10.1002/cite.201200179, 2013.

[3] UN, The Paris Agreement [WWW Document], United Nations - climate action, 2022. URL, https://www.un.org/en/climatechange/paris-agreement, 11.8.22.

[4] G. Iyer, Y. Ou, J. Edmonds, A.A. Fawcett, N. Hultman, J. McFarland, J. Fuhrman, S. Waldhoff, H. McJeon, Ratcheting of climate pledges needed to limit peak global warming, Nat. Clim. Change 12 (2022) 1129–1135, https://doi.org/10.1038/s41558-022-01508-0.

[5] K. Abbass, M.Z. Qasim, H. Song, M. Murshed, H. Mahmood, I. Younis, A review of the global climate change impacts, adaptation, and sustainable mitigation measures, Environ. Sci. Pollut. Control Ser. (2022), https://doi.org/10.1007/s11356-022-19718-6.

[6] L. Berrang-Ford, A.R. Siders, A. Lesnikowski, A.P. Fischer, M.W. Callaghan, N. R. Haddaway, K.J. Mach, M. Araos, M.A.R. Shah, M. Wannewitz, D. Doshi, T. Leiter, C. Matavel, J.I. Musah-Surugu, G. Wong-Parodi, P. Antwi-Agyei, I. Ajibade, N. Chauhan, W. Kakenmaster, C. Grady, V.I. Chalastani, K. Jagannathan, E.K. Galappaththi, A. Sitati, G. Scarpa, E. Totin, K. Davis, N.C. Hamilton, C. J. Kirchhoff, P. Kumar, B. Pentz, N.P. Simpson, E. Theokritoff, D. Deryng, D. Reckien, C. Zavaleta-Cortijo, N. Ulibarri, A.C. Segnon, V. Khavhagali, Y. Shang, L. Zvobgo, Z. Zommers, J. Xu, P.A. Williams, I.V. Canosa, N. van Maanen, B. van Bavel, M. van Aalst, L.L. Turek-Hankins, H. Trivedi, C.H. Trisos, A. Thomas, S. Thakur, S. Templeman, L.C. Stringer, G. Sotnik, K.D. Sjostrom, C. Singh, M. Z. Siña, R. Shukla, J. Sardans, E.A. Salubi, L.S. Safaee Chalkasra, R. Ruiz-Díaz, C. Richards, P. Pokharel, J. Petzold, J. Penuelas, J. Pelaez Avila, J.B.P. Murillo, S. Ouni, J. Niemann, M. Nielsen, M. New, P. Nayna Schwerdtle, G. Nagle Alverio, C.A. Mullin, J. Mullenite, A. Mosurska, M.D. Morecroft, J.C. Minx, G. Maskell, A. M. Nunbogu, A.K. Magnan, S. Lwasa, M. Lukas-Sithole, T. Lissner, O. Lilford, S. F. Koller, M. Jurjonas, E.T. Joe, L.T.M. Huynh, A. Hill, R.R. Hernandez, G. Hegde, T. Hawxwell, S. Harper, A. Harden, M. Haasnoot, E.A. Gilmore, L. Gichuki, A. Gatt, M. Garschagen, J.D. Ford, A. Forbes, A.D. Farrell, C.A.F. Enquist, S. Elliott, E. Duncan, E. Coughlan de Perez, S. Coggins, T. Chen, D. Campbell, K.E. Browne, K. J. Bowen, R. Biesbroek, I.D. Bhatt, R. Bezner Kerr, S.L. Barr, E. Baker, S.E. Austin, I. Arotoma-Rojas, C. Anderson, W. Ajaz, T. Agrawal, T.Z. Abu, A systematic global stocktake of evidence on human adaptation to climate change, Nat. Clim. Change 11 (2021) 989–1000, https://doi.org/10.1038/s41558-021-01170-y.

[7] S.K. Saraswat, A.K. Digalwar, S.S. Yadav, G. Kumar, MCDM and GIS based modelling technique for assessment of solar and wind farm locations in India, Renew. Energy 169 (2021) 865–884, https://doi.org/10.1016/j.renene.2021.01.056.

[8] IRENA, Global Energy Transformation: a Roadmap to 2050, 2018 (Abu Dhabi).

[9] M. Uyan, GIS-based solar farms site selection using analytic hierarchy process (AHP) in Karapinar region Konya/Turkey, Renew. Sustain. Energy Rev. (2013), https://doi.org/10.1016/j.rser.2013.07.042.

[10] P. Bojek, Solar PV [WWW document], Solar PV (2022). URL, https://www.iea.org/reports/solar-pv, 11.8.22.

[11] IEA, World Energy Outlook 2022, 2022.

[12] Republic of Turkey Ministry of Energy and Natural Resources, Electricity [WWW Document], Electricity, 2022. URL, https://enerji.gov.tr/infobank-energy-electricity, 11.8.22.

[13] Republic of Turkey Ministry of Energy and Natural Resources, Solar Energy [WWW Document], Solar energy, 2022. URL, https://enerji.gov.tr/bilgi-merkezi-enerji-gunes-en, 11.11.22.

[14] Republic of Turkey Ministry of Energy and Natural Resources, Biomass [WWW Document], Biomass, 2022. URL, https://enerji.gov.tr/bilgi-merkezi-enerji-biyokutle-en, 11.11.22.

[15] T. Höfer, Y. Sunak, H. Siddique, R. Madlener, Wind farm siting using a spatial Analytic Hierarchy Process approach: a case study of the Städteregion Aachen, Appl. Energy 163 (2016) 222–243, https://doi.org/10.1016/j.apenergy.2015.10.138.

[16] A.A. Merrouni, E.F. Elalaoui, Ahmed Mezrhab, Abdelhamid Mezrhab, A. Ghennioui, Large scale PV sites selection by combining GIS and Analytical Hierarchy Process. Case study: eastern Morocco, Renew. Energy 119 (2018) 863–873, https://doi.org/10.1016/j.renene.2017.10.044.

[17] A. Demir, A.E. Dinçer, K. Yılmaz, A novel method for the site selection of large-scale PV farms by using AHP and GIS: a case study in İzmir, Türkiye, Sol. Energy 259 (2023) 235–245, https://doi.org/10.1016/j.solener.2023.05.031.

[18] A.J. Carrión, A. Espín Estrella, F. Aznar Dols, M. Zamorano Toro, M. Rodríguez, A. Ramos Ridao, Environmental decision-support systems for evaluating the carrying capacity of land areas: optimal site selection for grid-connected photovoltaic power plants, Renew. Sustain. Energy Rev. (2008), https://doi.org/10.1016/j.rser.2007.06.011.

[19] J.M. Sánchez-Lozano, J. Teruel-Solano, P.L. Soto-Elvira, M. Socorro García-Cascales, Geographical Information Systems (GIS) and Multi-Criteria Decision Making (MCDM) methods for the evaluation of solar farms locations: case study in south-eastern Spain, Renew. Sustain. Energy Rev. (2013), https://doi.org/10.1016/j.rser.2013.03.019.

[20] M. Tahri, M. Hakdaoui, M. Maanan, The evaluation of solar farm locations applying Geographic Information System and Multi-Criteria Decision-Making methods: case study in southern Morocco, Renew. Sustain. Energy Rev. (2015), https://doi.org/10.1016/j.rser.2015.07.054.

[21] H.E. Colak, T. Memisoglu, Y. Gercek, Optimal site selection for solar photovoltaic (PV) power plants using GIS and AHP: a case study of Malatya Province, Turkey, Renew. Energy 149 (2020) 565–576, https://doi.org/10.1016/j.renene.2019.12.078.

[22] Y. Charabi, A. Gastli, PV site suitability analysis using GIS-based spatial fuzzy multi-criteria evaluation, Renew. Energy 36 (2011) 2554–2561, https://doi.org/10.1016/j.renene.2010.10.037.

[23] A. Aly, S.S. Jensen, A.B. Pedersen, Solar power potential of Tanzania: identifying CSP and PV hot spots through a GIS multicriteria decision making analysis, Renew. Energy 113 (2017) 159–175, https://doi.org/10.1016/j.renene.2017.05.077.

[24] D. Doljak, G. Stanojević, Evaluation of natural conditions for site selection of ground-mounted photovoltaic power plants in Serbia, Energy 127 (2017) 291–300, https://doi.org/10.1016/j.energy.2017.03.140.

[25] A. Suuronen, A. Lensu, M. Kuitunen, R. Andrade-Alvear, N.G. Celis, M. Miranda, M. Perez, J.V.K. Kukkonen, Optimization of photovoltaic solar power plant locations in northern Chile, Environ. Earth Sci. 76 (2017), https://doi.org/10.1007/s12665-017-7170-z.

[26] S.N. Shorabeh, M.K. Firozjaei, O. Nematollahi, H.K. Firozjaei, M. Jelokhani-Niaraki, A risk-based multi-criteria spatial decision analysis for solar power plant site selection in different climates: a case study in Iran, Renew. Energy 143 (2019) 958–973, https://doi.org/10.1016/j.renene.2019.05.063.

[27] Y. Noorollahi, A. Ghenaatpisheh Senani, A. Fadaei, M. Simaee, R. Moltames, A framework for GIS-based site selection and technical potential evaluation of PV solar farm using Fuzzy-Boolean logic and AHP multi-criteria decision-making approach, Renew. Energy 186 (2022) 89–104, https://doi.org/10.1016/j.renene.2021.12.124.

[28] IPCC, Global Warming of 1.5°C, Global Warming of 1.5°C, Cambridge University Press, 2022, https://doi.org/10.1017/9781009157940.

[29] T.L. Saaty, K. Kułakowski, Axioms of the Analytic Hierarchy Process (AHP) and its generalization to dependence and geedback: the analytic network Process (ANP), ArXiv 1 (2016) 1–12, https://doi.org/10.48550/arXiv.1605.05777.

[30] T.L. Saaty, Decision making with the analytic hierarchy process, Int. J. Services Sciences 1 (2008) 83–98.

[31] O.S. Vaidya, S. Kumar, Analytic hierarchy process: an overview of applications, Eur. J. Oper. Res. 169 (2006) 1–29, https://doi.org/10.1016/j.ejor.2004.04.028.

[32] G.A. Miller, A. Baddeley, R.M. Shiffrin, R.M. Nosofsky, The magical number seven, plus or minus two: some limits on our capacity for processing information, Psychol. Rev. (1994).

[33] T.L. Saaty, Decision Aiding Decision-making with the AHP: why is the principal eigenvector necessary, Eur. J. Oper. Res. 145 (2003) 85–91.

[34] E. Noorollahi, D. Fadai, M.A. Shirazi, S.H. Ghodsipour, Land suitability analysis for solar farms exploitation using GIS and fuzzy analytic hierarchy process (FAHP) - a case study of Iran, Energies 9 (2016), https://doi.org/10.3390/en9080643.

[35] J. Domínguez Bravo, X. García Casals, I. Pinedo Pascua, GIS approach to the definition of capacity and generation ceilings of renewable energy technologies, Energy Pol. 35 (2007) 4879–4892, https://doi.org/10.1016/j.enpol.2007.04.025.

[36] M.A. Günen, A comprehensive framework based on GIS-AHP for the installation of solar PV farms in Kahramanmaraş, Turkey, Renew. Energy 178 (2021) 212–225, https://doi.org/10.1016/j.renene.2021.06.078.

[37] L. Alfieri, B. Bisselink, F. Dottori, G. Naumann, A. de Roo, P. Salamon, K. Wyser, L. Feyen, Global projections of river flood risk in a warmer world, Earth's Future 5 (2017) 171–182, https://doi.org/10.1002/2016EF000485.
[38] L.J. Slater, G. Villarini, Recent trends in U.S. flood risk, Geophys. Res. Lett. 43 (2016), https://doi.org/10.1002/2016GL071199, 12,428-12,436.
[39] Intergovernmental Panel on Climate Change (IPCC), Global warming of 1.5°C. Special report. NYC: IPCC, in: Global Warming of 1.5°C, Cambridge University Press, 2019, https://doi.org/10.1017/9781009157940.003.
[40] A. Demir, Hydro-elastic analysis of standing submerged structures under seismic excitations with sph-fem approach, Lat. Am. J. Solid. Struct. 17 (2020) 1–14, https://doi.org/10.1590/1679-78256266.
[41] A. Demir, A.E. Dinçer, Ş. Öztürk, İ. Kazaz, Numerical and experimental investigation of sloshing in a water tank with a fully coupled fluid-structure interaction method, Prog. Comput. Fluid Dynam. Int. J. 21 (2021) 103–114, https://doi.org/10.1504/PCFD.2021.113675.
[42] A.E. Dinçer, A. Demir, Z. Bozkus, A.S. Tijsseling, Fully coupled smoothed particle hydrodynamics-finite element method approach for fluid-structure interaction problems with large deflections, Journal of Fluids Engineering, Transactions of the ASME 141 (2019), https://doi.org/10.1115/1.4043058.
[43] K. Yilmaz, Y. Darama, Y. Oruc, A.B. Melek, Assessment of flood hazards due to overtopping and piping in Dalaman Akköprü Dam, employing both shallow water flow and diffusive wave equations, Nat. Hazards 117 (2023) 979–1003, https://doi.org/10.1007/s11069-023-05891-5.
[44] D.C. Froehlich, Peak outflow from breached embankment dam, J. Water Resour. Plann. Manag. 121 (1995) 90–97.
[45] K. Yılmaz, A.E. Dinçer, V. Kalpakcı, Ş. Öztürk, Debris flow modelling and hazard assessment for a glacier area: a case study in Barsem, Tajikistan, Nat. Hazards 115 (2023) 2577–2601, https://doi.org/10.1007/s11069-022-05654-8.
[46] W.H. Wicschmeier, D.D. Smith, Predicting Rainfall Erosion Losses: a Guide to Conservation Planning, U.S. Department of Agriculture, 1978.
[47] K.G. Renard, G.R. Foster, G.A. Weesies, D.K. McCool, D.C. Yoder, Predicting soil erosion by water: a guide to conservation planning with the revised universal soil loss equation (RUSLE), handbook No. 703, in: U.S. Department of Agriculture, 1997.
[48] P. Borrelli, M. Märker, P. Panagos, B. Schütt, Modeling soil erosion and river sediment yield for an intermountain drainage basin of the Central Apennines, Italy, Catena 114 (2014) 45–58, https://doi.org/10.1016/j.catena.2013.10.007.
[49] I.D. Moore, G.J. Burch, Physical basis of the length-slope factor in the universal soil loss equation, Soil Sci. Soc. Am. L. 50 (1986) 1294–1298.
[50] H.R. Naqvi, J. Mallick, L.M. Devi, M.A. Siddiqui, Multi-temporal annual soil loss risk mapping employing revised universal soil loss equation (RUSLE) model in nun nadi watershed, Uttrakhand (India), Arabian J. Geosci. 6 (2013) 4045–4056, https://doi.org/10.1007/s12517-012-0661-z.
[51] S. Pelacani, M. Märker, G. Rodolfi, Simulation of soil erosion and deposition in a changing land use: a modelling approach to implement the support practice factor, Geomorphology 99 (2008) 329–340, https://doi.org/10.1016/j.geomorph.2007.11.010.
[52] A.A. Fenta, H. Yasuda, K. Shimizu, N. Haregeweyn, A. Negussie, Dynamics of soil erosion as influenced by watershed management practices: a case study of the Agula watershed in the semi-arid highlands of Northern Ethiopia, Environ Manage 58 (2016) 889–905, https://doi.org/10.1007/s00267-016-0757-4.
[53] B. Song, S. Kang, A method of assigning weights using a ranking and nonhierarchy comparison, Adv. Dec. Sci. 2016 (2016), https://doi.org/10.1155/2016/8963214.
[54] Smith GP, Davey EK, Cox RJ (2014) Flood hazard, WRL technical report 2014/07, WRL Tech. Rep. 2014/07, no. September, p 59. https://knowledge.aidr.org.au/media/2334/wrl-flood-hazard-techinical-report-september-2014.pdf.
[55] Meteoroloji Genel Müdürlüğü (MGM), [WWW Document], 2022 URL https://www.mgm.gov.tr/veridegerlendirme/il-ve-ilceler-istatistik.aspx?m=MUGLA 11.11.22.
[56] Devlet Planlama Teşkilatı (DPT), Sekizinci Beş Yıllık Kalkınma Planı, Tarımsal Politikalar ve Yapısal Düzenmeler Özel İhtisas Komisyonu Raporu, 2001, 67 Sayfa.